



Sharif University of Technology

Scientia Iranica

Transactions B: Mechanical Engineering

<https://scientiairanica.sharif.edu>

# Numerical simulation of water drop deformation under electrical fields in oil fields

M. Taghian<sup>a</sup> and S. Yaghoubi<sup>a,b,\*</sup><sup>a</sup>. Department of Mechanical Engineering, Najafabad Branch, Islamic Azad University, Najafabad, Iran.<sup>b</sup>. Aerospace and Energy Conversion Research Center, Najafabad Branch, Islamic Azad University, Najafabad, Iran.

Received 7 August 2022; received in revised form 21 November 2022; accepted 15 August 2023

## KEYWORDS

Two-phase flow;  
Electrical field;  
Earth's gravity;  
Water drop  
deformation;  
Separating  
electro-filter.

**Abstract.** The separation of a fluid from an immiscible liquid can be used in many natural ways. Traditional methods are currently used to accomplish this process. In this study, we attempted to investigate the effect of changes in the geometric radius of the water droplet in the oil medium and applied voltage to provide outputs that can be used to better design water separating electro-filter for crude oil. Furthermore, the most important innovation of this article is to study considering the effects of the presence and absence of Earth's gravity. The results of this work show that changes in geometry and voltage were effective in the deformation and movement of the drops, but their effects were not significant compared to the presence and absence of gravity. In other words, the effect of considering Earth's gravity in this study tends to make the results realistic, and the results would not be comparable to those obtained in the absence of Earth's gravity.

© 2024 Sharif University of Technology. All rights reserved.

## 1. Introduction

Due to the reduction of fossil energies such as oil and gas and the pollution caused by the consumption of these fuels [1,2], nowadays the use of renewable energies has been considered to meet the energy needs [3,4]. In the future, energy and the environment are the two main concerns, and it is essential to develop sustainable renewable energy technologies [5,6]. However, in many countries, they still use oil and gas sources to supply their energy needs [7,8].

Nowadays, an attempt is made to prevent an unfortunate incident in the industry, which is the chaining of water molecules. Because this may lead to terrible explosions [9,10].

The electrohydrodynamics (EHD) of drops and

emulsions is of great importance due to its far-ranging practical applications in several industrial processes such as emulsification, atomization, enhanced heat transfer, enhanced coalescence, and phase separation of water from crude oil [11,12]. With the advent of modern-day small-scale devices, fine-tuned manipulation of drops is achieved by the application of an external electric field [13,14]. In the above-mentioned applications, the drops encounter the simultaneous presence of imposed hydrodynamic flow and electric fields [15,16].

A droplet suspended in another immiscible fluid will deform under an externally applied electric field. Applications of this phenomenon encompass electrospinning [17], electrospraying [18], electrostatic coalescence of droplets for emulsification purposes [19,20], and electrowetting-based droplet manipulation in microfluidic systems [21], to name a few.

For a better understanding of droplet deformation under the influence of an electric field, some experimental and numerical research has been conducted from different perspectives [22,23]. The mathematical

\* Corresponding author.

E-mail addresses: [m.taghian1994@gmail.com](mailto:m.taghian1994@gmail.com) (M. Taghian); [s.yaghoubi@pmc.iaun.ac.ir](mailto:s.yaghoubi@pmc.iaun.ac.ir) (S. Yaghoubi)

description of this phenomenon has been established, and some aspects of the equilibrium and transient process under different types of electric fields have been substantially investigated [24,25].

Recently Huang et al. [26] worked on the deformation and coalescence behaviors of water droplets with experiments and numerical simulations. This study is done in a viscous fluid under a direct current electric field. The electrocoalescence process of water droplet trains in sunflower oil under the coupling effect is experimentally investigated by Li et al. [27] in two states: non-uniform electric and laminar flow fields. Also, they numerically investigate the electrocoalescence of an aqueous droplet at the oil-water interface [28]. They analyze this problem in the presence of externally direct current electric fields and solve the Navier-Stokes equations with the finite element method.

In [29], the deformation of droplets in the oil field was studied with a special type of electric field, Chaotic Pulse Position Modulation (CPPM) electric field, and its dynamics model was developed. The electric field intensity and pulse width were investigated. They found that increasing the pulse width leads to a decrease in the chaos of droplet deformation.

In [30], the breakup and deformation of the water droplet are studied in acidic crude oil and a uniform electric field using a molecular dynamics method. They used an MD method to investigate a single water droplet behavior at different field strengths. In this research, they understood that naphthenic acid formed a strong hydrogen bond (H-bond) with water in weak interaction. On naphthenic acid, the carboxyl group was mainly attracted via interaction on the surface of the droplet.

In [31], molecular dynamics simulation was used to discover mechanisms of deformation and breakup of the water droplet in oil and the effect of the strength of the electric field on the dynamics of that. Their results proved that the Solvent Accessible Surface Area (SASA) in addition to the Deformation Ratio (DR), is a very important parameter to determine the degree of droplet deformation at the molecular level.

In [32], a methodology is represented to investigate the bubbles and drops in incompressible flows with the effect of surface tension. It is a combination of the immersed interface method and the Level Set (LS) method. To resolve discontinuities and reproduce the evolving interfaces, respectively.

All of the above-mentioned studies are generally limited to the analysis of steady and unsteady states of liquid drops under electrical fields and their results are not focused on the transition conditions of droplet deformation. A transitional response of deformed drops to electrical fields is closely correlated to their surface characteristics and can be used for describing these characteristics and discovering the main factors affect-

ing these deformations. However, transition responses of drops to an external electrical field have rarely been investigated. In this study, we attempted to investigate the effect of changes in the geometric radius of the water droplet in the oil medium and applied voltage to provide outputs that can be used to better design water separating electro-filter for crude oil. Furthermore, the most important innovation of this article is to study considering the effects of the presence and absence of Earth's gravity. The results of this work show that changes in geometry and voltage were effective in the deformation and movement of the drops, but their effects were not significant compared to the presence and absence of gravity. In other words, the effect of considering Earth's gravity in this study tends to make the results realistic, and the results would not be comparable to those obtained in the absence of Earth's gravity.

In the following, the description of the problem was done. Also, the method and governing equations were defined and the last part discussed the results, validation of them, and their analysis.

## 2. Problem description

Filters are often used to remove solids which are suspended in a fluid and are one of the main industrial processes. The need for filtration and separation of immiscible phases is one of the main needs in different sectors of the industry and therefore, filtering is one of the phenomena that are of interest to basic research [33].

The separation of immiscible liquids by the natural method cannot be sufficiently significant. The separation process can therefore be enhanced by partial excitation between the droplets using mechanical, thermal, electromagnetic, or other forces [34].

Usually, low-efficiency separators are used in the filtering process using additives that are effective for mechanically separating or smoothing coarse particles. Therefore, the desire to create new and optimal ways to separate non-miscible fluids such as petroleum, oil, and grease solutions has been considered [35].

The use of an electric field is a prospective approach for the separation of immiscible fluids in the separation process. These filters are known as electro-filters. An electro-filter is a device that separates particles in the fluid by creating an electric field. The advantage of this filter over other filters is reducing the pressure drop in the fluid flow path. Furthermore, the separation efficiency of particles smaller than one micron in this type of filter is higher than in other filters. Therefore, this method has received more attention than others. Despite lower power consumption, this type of filter separates unmixed fluids in a shorter time and with higher efficiency.

In general, the purpose of this study was to

numerically simulate the behavior of water droplets in the oil field in the presence of an electric field using the COMSOL Multiphysics software which is created and deformed due to the bipolarity of the water.

The initial studies on the deformation of an insulating droplet suspended in another immiscible fluid indicated the existence of forces perpendicular to the interface and finally the deformation of the droplet in the form of prolate (stretching in the direction of the field). O’Konski and Thacher Jr [36], while obtaining a relation for the deformation of a liquid droplet suspended in another insulating fluid, talked about its deformation in the direction of the electric field.

Also, Taylor [37], by examining the breakdown of water droplets in an electric field experimentally, reported their coning (stretching in the direction of the electric field) before breaking. Basaran and Scriven [38] simulated the final shape of a conductive droplet suspended in an insulating fluid with the Galerkin finite element method and stated that this droplet changes shape in a conical shape (stretching in the direction of the electric field).

However, the experiments of Allan and Mason [39] showed the existence of oblate deformation (stretching in the direction perpendicular to the field direction). In this way, there is no completely insulating fluid in nature, and even the presence of small conductivity in the main fluid causes the transfer of loads to the interface. The result of this charge transfer is the creation of tangential stresses and fluid movement along the borders of the drop, which ultimately leads to the creation of circulation currents inside and outside the drop. The direction of these currents depends on the ratio of electric conductivity and electric permeability of the drop and the surrounding fluid, and their intensity depends on the strength of the electric field.

Reducing the amount of water in crude oil, especially when entering into pipes and for export, is essential. Therefore, improving the timing and speed of water separation from crude oil is important. This process requires a greater understanding of the coagulation mechanism under the electric field.

### 3. Research and modeling method

#### 3.1. Equations governing research

The equations governing this problem include three essential parts. Navier-Stokes equations are used for solving the hydrodynamic equations; the LS approach is used for modeling the interface between two phases and electrical field equations are used to calculate the forces applied to the droplet.

Based on these facts, in the problem of separating water from petroleum compounds, the discrete phase (water) is carried by the oil. Therefore, the problem

will include two main elements; the petroleum phase which is a continuous phase, and water droplets which should be investigated as a discrete phase. Therefore, the solution model must be divided into two parts for each element.

##### 3.1.1. Maxwell stress tensor

Maxwell stress tensor can be calculated using the following equation:

$$t^e = \varepsilon \varepsilon_0 (\vec{E} \cdot \vec{E} - \frac{1}{2} \vec{E} \vec{E}). \quad (1)$$

While the electrical force applied to the unit of volume is calculated using the following equation:

$$F^e = \nabla \cdot t^e = -\frac{1}{2} (\vec{E} \cdot \vec{E} \nabla \varepsilon + q^v \vec{E}). \quad (2)$$

Maxwell’s electrical stress is applied to the phase interface and is always perpendicular to the interface and, if there are no other stresses, results in the droplet being stretched along the electrical field [40]. Electrical forces are the volumetric forces resulting from non-zero charge density at each point in the fluid’s volume. These stresses can result in the droplet being deformed to a flat elliptical along the electrical fields. Deformation of the droplet in the electrical field is the result of interactions between electrical stress, surface tension as well as viscosity and inertia forces of two fluids.

##### 3.1.2. Hydrodynamic equations

The hydrodynamic problem can be described using continuum equations as well as Navier-Stokes incompressible flow equations:

$$\rho \frac{\partial \vec{V}}{\partial t} + \rho (\vec{V} \cdot \nabla) \vec{V} = -\nabla P + \nabla \cdot \left( \mu \left\langle \nabla \vec{V} + (\nabla \vec{V})^T \right\rangle \right) + f_g + F^e, \quad (3)$$

$$\nabla \cdot \vec{V} = 0. \quad (4)$$

If the fluid is assumed to be Newtonian in nature, the fluid’s viscosity,  $\mu$ , can be considered as a scalar value and since the droplets being investigated are very small, the effect of gravity on them can be neglected. This assumption is used in most important works in this regard [41,42]. Furthermore, in this equation,  $\vec{V}$  is the velocity vector. Without the presence of free shares on the interface, the electrical force term will be the only boundary term. Therefore, no significant volumetric forces exist and the right side of the equation will be equal to zero [43].

##### 3.1.3. Interface (LS) equations

In the current study, the LS approach is used to follow the interface. This method was first introduced by

Osher and Sethian [44] and has seen ever-increasing use due to its ability to model complex surfaces as well as its intrinsic smoothness. The basic idea of this method is considering a continuous scalar function  $\phi$ . The interface between two fluids is known with a zero value of  $\phi$  while  $\phi > 0$  shows one side of the interface and  $\phi < 0$  indicates the other side of the interface. The equation will then be as follows:

$$\frac{\partial \phi}{\partial t} + u \cdot (\nabla \phi) = \gamma \nabla \cdot \left( \varepsilon_{ls} \nabla \phi - \phi(1 - \phi) \frac{\nabla \phi}{|\nabla \phi|} \right). \quad (5)$$

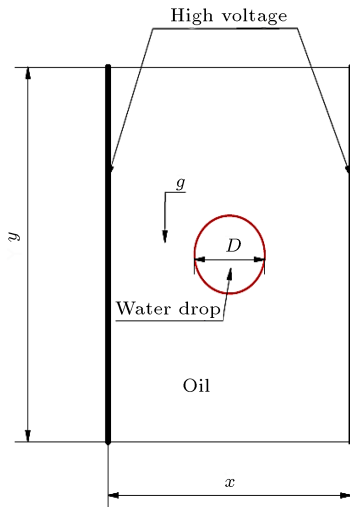
In this equation,  $t$  indicates the time,  $u$  is the velocity field, and the  $\varepsilon_{ls}$  shows the interface thickness. When stabilization is used in this equation, the thickness of the interface can often be described as  $\varepsilon_{ls} = h_c/2$  in which  $h_c$  is the mesh size of the interface. Finally,  $\gamma$  parameters are the initial values, the best value for which is the maximum velocity in the model.

### 3.2. Assumptions and boundary conditions

In this study, an oil container is considered inside of which a water drop is placed. Two electrodes are placed on both sides of the container which are connected to positive and negative voltage sources. The geometrical dimensions are determined after initial simulations to optimize the effect of the electrical field on the water drop and the problem is solved in two dimensions. The following schematic shows the geometry of the problem (Figure 1).

According to this schematic, the wall boundary conditions are considered for all four boundaries, and two boundaries on the left and right sides are connected to the electrical potential source. The initial conditions and assumptions used in the solution are as follows:

- The water drop is initially floating inside the oil;
- Due to constant temperature, the emulsion properties are considered to be constant;



**Figure 1.** The schematic of the geometry of the problem.

- Lagrangian-Eulerian flow model at the water and oil interface is used for simulations;
- The diameter of the water drop and the strength of the applied electrical field are investigated as dependent variables of the problem;
- Simulation is analyzed during the stop time of the fluid.

Figure 2(a) shows the schematic of the geometrical model created in COMSOL software. All units are based on mm and deg, creating a rectangle with dimensions of 50 mm to 100 mm for the oil container, with the circle in the middle indicating the water drop. These dimensions were selected based on previous studies.

The software uses its existing functions at the temperature of 293.15 K to determine mechanical characteristics such as CP, dynamic viscosity, and density of water and oil. Table 1 shows the properties used for the simulation of water and oil. Furthermore, the problem is solved as a time-dependent problem.

#### 3.2.1. Initial and boundary conditions of the electrical field

According to Figure 2(b), the upper and lower boundaries of the container have electrical insulation conditions in order to create a uniform electrical field moving from right to left.

The source of electrical potential is located on the right side of the container and the left side is the earth connection.

#### 3.2.2. Initial and boundary conditions of the fluids

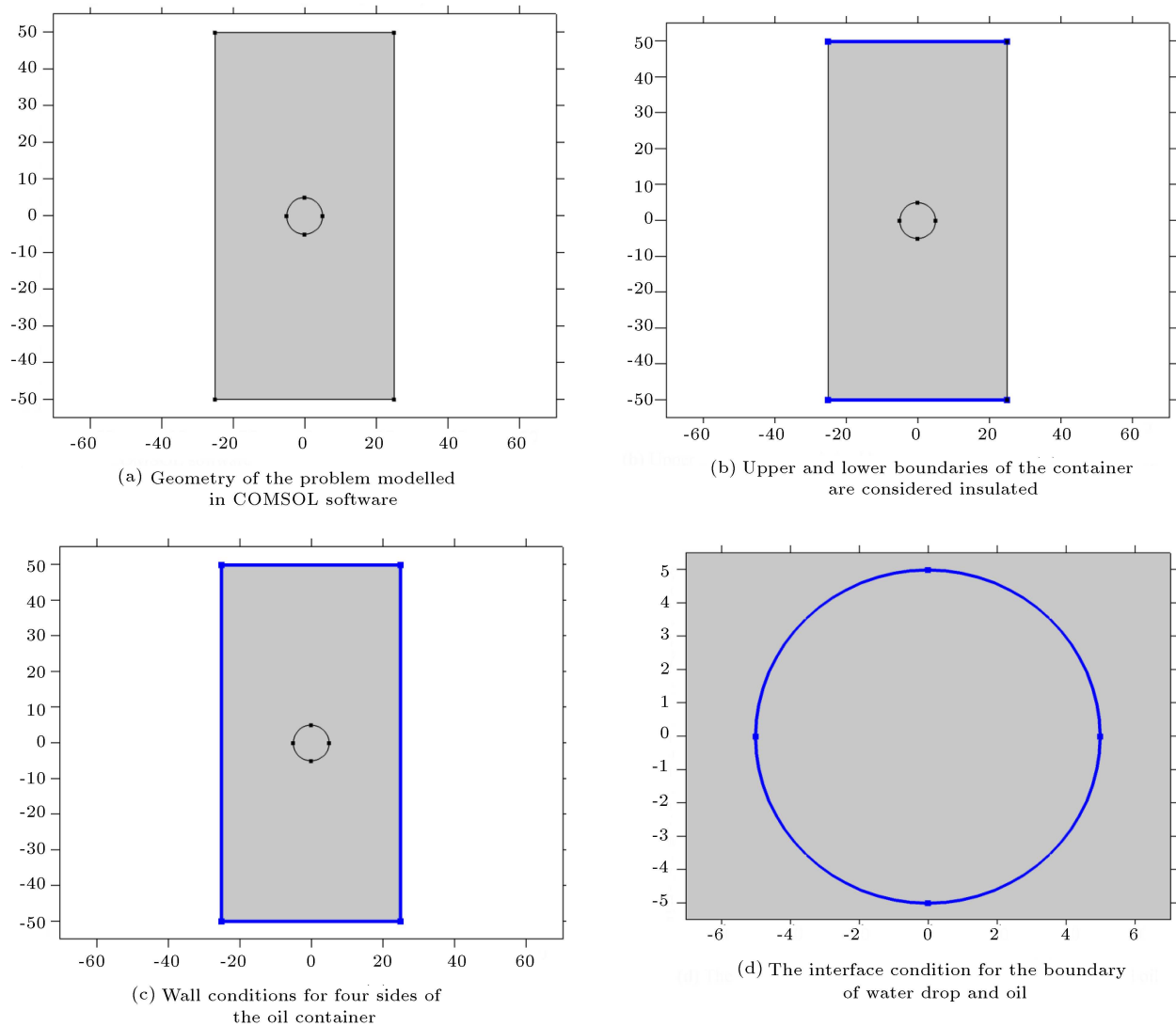
As shown in Figure 2(c), four wall boundary conditions are defined on all four sides of the container. Therefore, the no-slip boundary condition applies to all four container boundaries.

As shown in Figure 2(d), the boundary between water drop and water is modeled as the interface condition.

In steps when the gravitational force is added to the equations, its value is considered equal to the universal constant defined by the software and is applied as  $-g$  in the vertical direction of the model. For the surrounding areas, the initial values of zero velocity and zero pressure are used.

**Table 1.** Properties of water drop and crude oil used in the simulations.

|            | Viscosity<br>(Pa.s) | Density<br>(kg/m <sup>3</sup> ) | Electrical<br>conductivity<br>coefficient |
|------------|---------------------|---------------------------------|---|
| Water drop | 0.0013              | 998.2                           | 80  |
| Crude oil  | 0.474               | 884                             | 2.2                                       |



**Figure 2.** Geometry and boundary conditions in simulating the problem.

#### 4. Validation

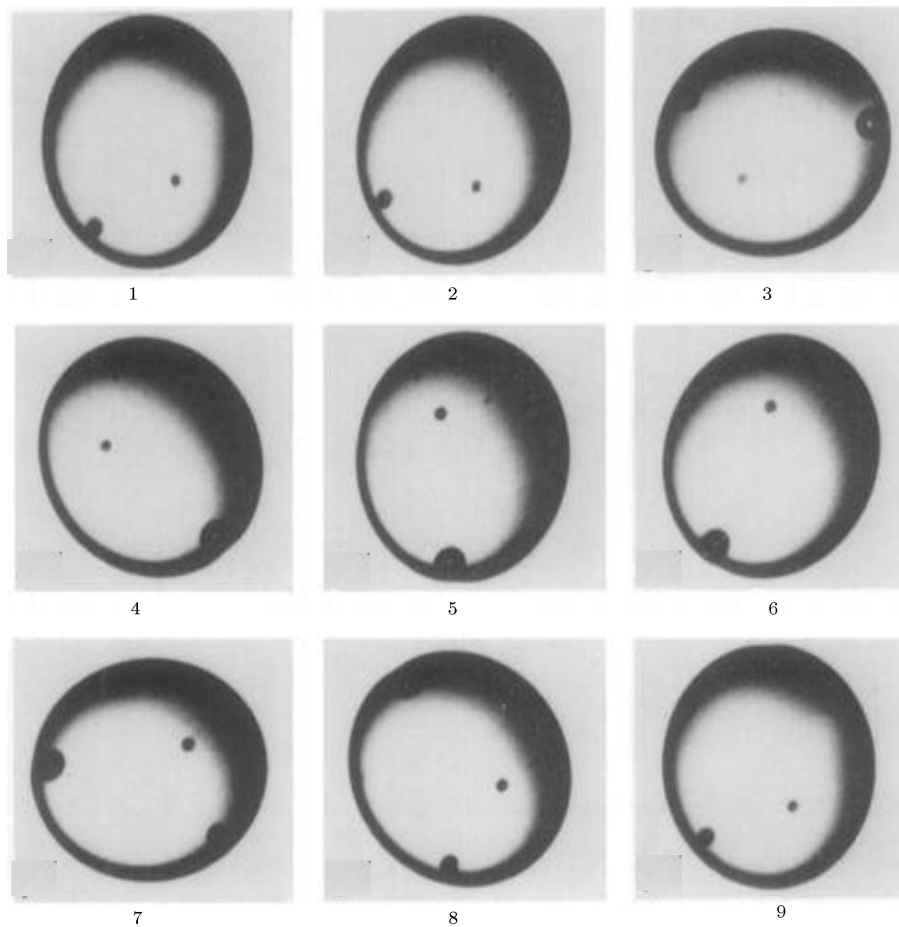
As can be seen in Figure 3, in this study, 9 experimental samples with different density conditions were affected by an electrical field, and deformation in the times between 0 to 5 seconds was empirically investigated. Since the target sample in this study was the water droplet, a sample with a density equal to that of water was used in numerical modeling using COMSOL software, and the extracted data was presented in comparative form (numerical/empirical) (Figure 4).

Based on the results extracted from numerical analysis and comparison with empirical data, it can be seen that the maximum deviation between these results is 15% observed at a time stamp of 4 seconds. An important fact is that both graphs follow logical progress until 3 seconds but after 3 seconds, deformation increases significantly due to similar alignment between the electrical field and water droplet conditions.

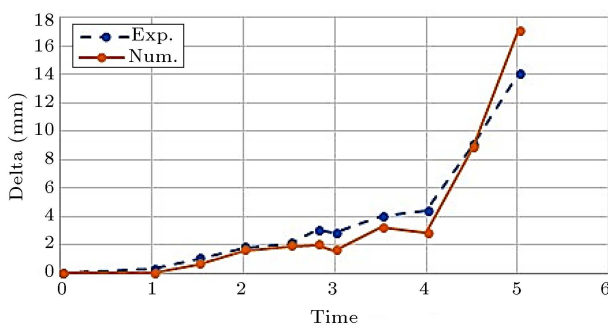
One of the important steps in this study is the validation step. To this end, the data provided in the experimental study by Torza et al. [45] in 1971 was used which showed the deformation of a drop in a two-phase environment. During the validation process, modeling information is extracted from previous studies (Figure 3), and after numerical modeling in the COMSOL software, the results are compared with previous data, and conclusions are provided. Data extracted after the numerical modeling process in COMSOL software indicate that the deviation between numerical outputs and experimental data is at most 15%. This deviation can be due to experimental errors in the empirical data and the use of ideal numbers during the numerical modeling of the problem.

#### 5. Result and discution

Based on the aim of the current study, the sample



**Figure 3.** Images of 9 different experimental samples showing changes under electrical field in a two-phase flow [37].



**Figure 4.** Comparison graph between empirical data and numerical analysis in COMSOL software.

model was analyzed and the results were evaluated. Since the main focus of the current study is to investigate the deformation of water droplets in an oil medium, the behavior of the droplet was first investigated under ideal conditions and then under the effect of the earth's gravity. Based on the strength of the electrical field in each case with or without the earth's gravity, the applied voltage is selected. The analyses carried out in COMSOL software based on problem solution conditions are presented in Table 2.

As can be seen in Table 2, all 24 analyses were

modeled using LS equations before analysis. Since the current study aims to compare the deformation of water droplets in oil media in the presence of electrical fields, the termination condition for analyses are as follows:

1. The impact between the droplet and the oil's boundaries;
2. The fracturing of the droplet, resulting in several drops in the oil medium.


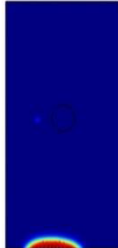
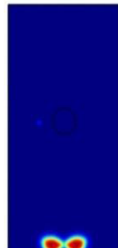
Based on these conditions, analyses were carried out and deformation and decentralization graphs for the water droplet in a two-phase environment were extracted (Table 3).

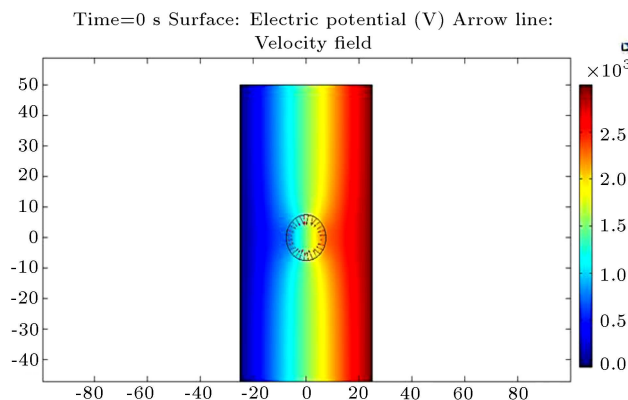
Based on the result presented in Table 4 for software analyses of a two-phase water and oil system for different conditions, it can be seen that under constant voltage and different diameters from 5 mm to 10 mm, deformation decreases even during movement of the water droplet. However, it is important to note that at constant diameters, deformation increases with an increase in the voltage and this can be seen even at a diameter of 10 mm.

**Table 2.** Details of analyses in the current study.

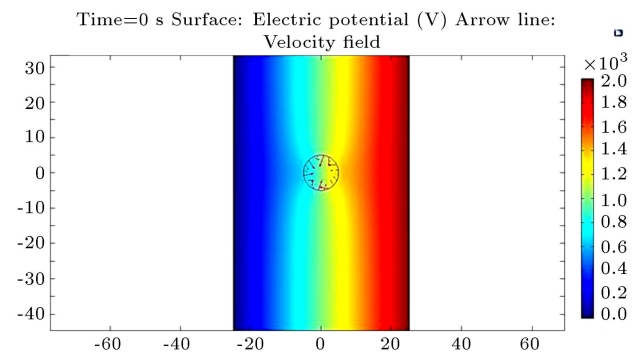
| Analyses details |                 |                 |                 |                 |                 |
|------------------|-----------------|-----------------|-----------------|-----------------|-----------------|
| Analysis 1.1     | Analysis 2.1    | Analysis 3.1    | Analysis 4.1    | Analysis 5.1    | Analysis 6.1    |
| Disable gravity  | Disable gravity | Disable gravity | Disable gravity | Disable gravity | Disable gravity |
| $R = 5$          | $R = 5$         | $R = 5$         | $R = 5$         | $R = 7.5$       | $R = 7.5$       |
| $V_0 = 1000$     | $V_0 = 2000$    | $V_0 = 3000$    | $V_0 = 5000$    | $V_0 = 1000$    | $V_0 = 2000$    |
| Analysis 1.2     | Analysis 2.2    | Analysis 3.2    | Analysis 4.2    | Analysis 5.2    | Analysis 6.2    |
| Enable gravity   | Enable gravity  | Enable gravity  | Enable gravity  | Enable gravity  | Enable gravity  |
| $R = 5$          | $R = 5$         | $R = 5$         | $R = 5$         | $R = 7.5$       | $R = 7.5$       |
| $V_0 = 1000$     | $V_0 = 2000$    | $V_0 = 3000$    | $V_0 = 5000$    | $V_0 = 1000$    | $V_0 = 2000$    |
| Analysis 7.1     | Analysis 8.1    | Analysis 9.1    | Analysis 10.1   | Analysis 11.1   | Analysis 12.1   |
| Disable gravity  | Disable gravity | Disable gravity | Disable gravity | Disable gravity | Disable gravity |
| $R = 7.5$        | $R = 7.5$       | $R = 10$        | $R = 10$        | $R = 10$        | $R = 10$        |
| $V_0 = 3000$     | $V_0 = 5000$    | $V_0 = 1000$    | $V_0 = 2000$    | $V_0 = 3000$    | $V_0 = 5000$    |
| Analysis 7.2     | Analysis 8.2    | Analysis 9.2    | Analysis 10.2   | Analysis 11.2   | Analysis 12.2   |
| Enable gravity   | Enable gravity  | Enable gravity  | Enable gravity  | Enable gravity  | Enable gravity  |
| $R = 7.5$        | $R = 7.5$       | $R = 10$        | $R = 10$        | $R = 10$        | $R = 10$        |
| $V_0 = 3000$     | $V_0 = 5000$    | $V_0 = 1000$    | $V_0 = 2000$    | $V_0 = 3000$    | $V_0 = 5000$    |

**Table 3.** Termination conditions during analyses of water droplets.

| Acceptance  | Termination Condition 1   | Termination Condition 2   |
|---|---|---|
|  |  |  |
| Acceptable condition  | Droplet impact termination condition  | Droplet fracture termination condition  |

**Figure 5.** Electrical field surrounding the water drop and distribution of electrical charges at  $t = 0$  s (A7.1)

Based on Table 4 and Figures 5 and 6, the movement direction of the water droplet is in the direction of the change in the electrical field, and the movement of a water droplet in the absence of gravity is only affected by the distribution of electrical charges along the interface between water and the surrounding

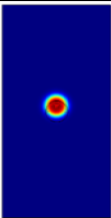
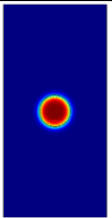
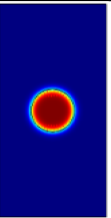
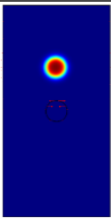
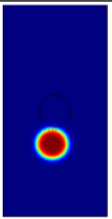
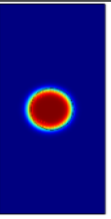
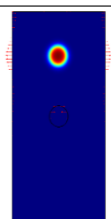
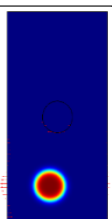
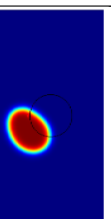
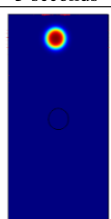
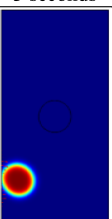
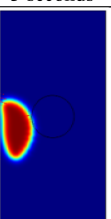
**Figure 6.** Electrical field surrounding the water drop and distribution of electrical charges at  $t = 3$  s (A7.1)

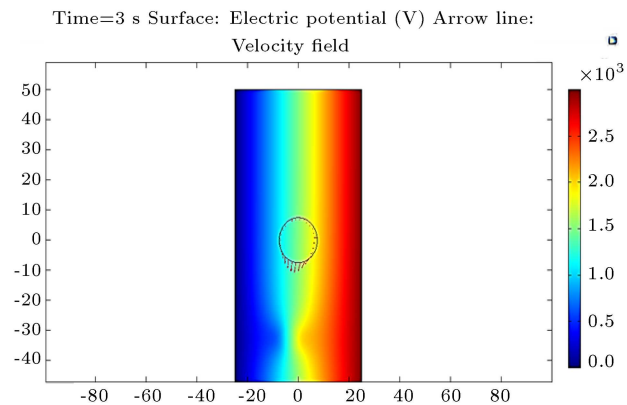
fluid; with free charges on the interface resulting in up and down movement in the droplet.

### 5.1. Droplet deformation in the absence of earth's gravity

Based on the result, in the absence of the earth's gravity; the analysis results are presented in Table 4. Furthermore, based on Table 3 and Figures 7 and 8 it

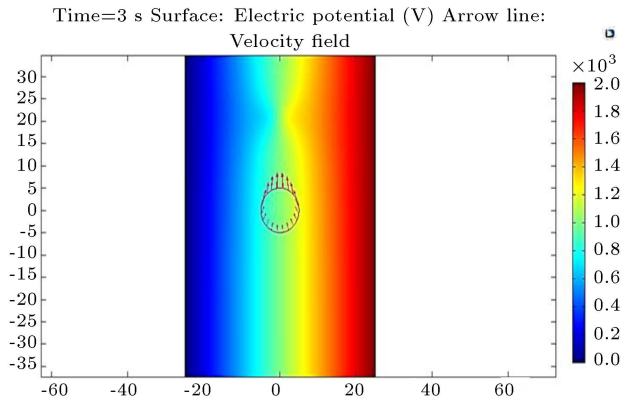
**Table 4.** The deformation results for the stopped-time shape in the absence of gravity.

| Voltage | Remarks | Drop radius   |   |   |
|---------|---------|---|---|---|
|         |         | 5 mm  | 7.5 mm  | 10 mm   |
| 1000    | Shape   |    |    |    |
|         | Time    | 3 seconds   | 3 seconds   | 3 seconds   |
| 2000    | Shape   |    |    |    |
|         | Time    | 3 seconds   | 3 seconds   | 3 seconds   |
| 3000    | Shape   |   |   |   |
|         | Time    | 3 seconds   | 3 seconds   | 3 seconds   |
| 5000    | Shape   |  |  |  |
|         | Time    | 3 seconds   | 3 seconds   | 3 seconds   |



**Figure 7.** Electrical field surrounding the water drop and distribution of electrical charges at  $t = 0$  s (A2.1)

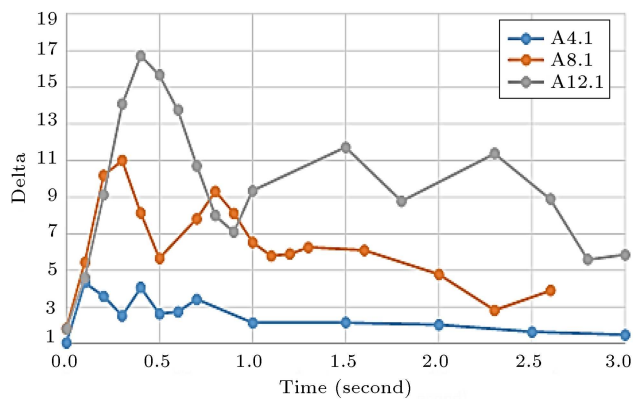
can be seen that the drop movement in A2.1 has been toward the direction of the change in the electrical field and has been affected by the charge distribution on the interface between the water drop and surrounding fluid.



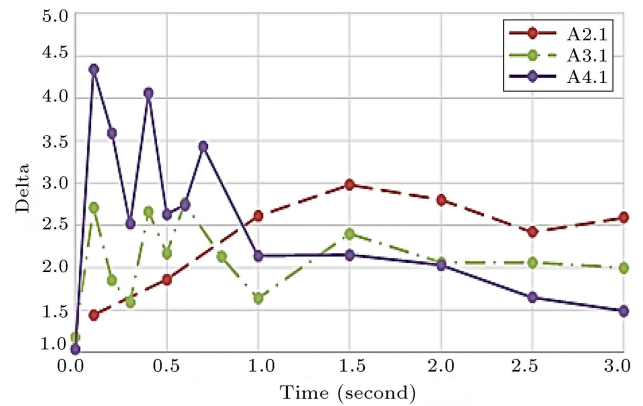
**Figure 8.** Electrical field surrounding the water drop and distribution of electrical charges at  $t = 3$  s (A7.1)

To provide a more precise analysis of the deformation parameter in the two-phase flow in the absence of gravity, it is necessary to develop numerical graphs based on regression analyses as presented in Figures 9,

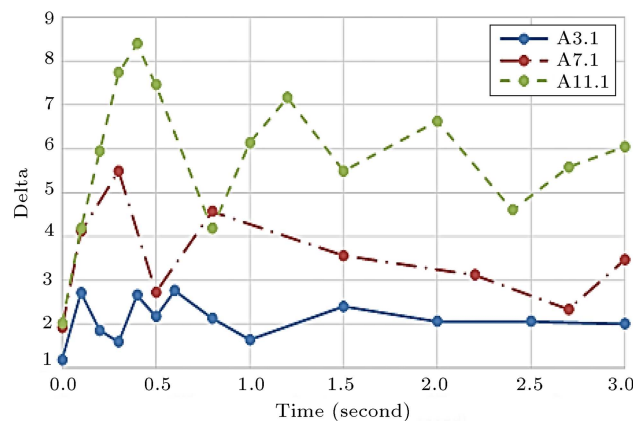




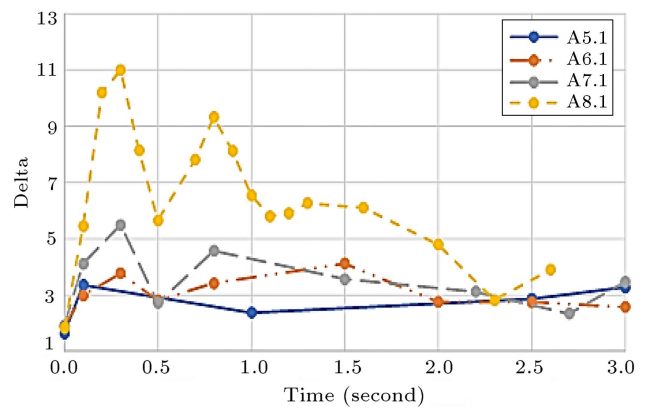
**Figure 9.** The graphs for water drop deformation in two-phase flow in the absence of gravity with a voltage of 5000 V.



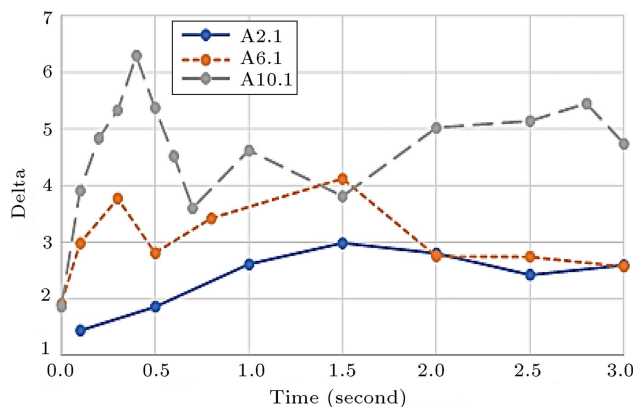
**Figure 12.** Water drop deformation graph for two-phase flow in the absence of gravity for a drop radius of 5 mm and variable applied voltage.



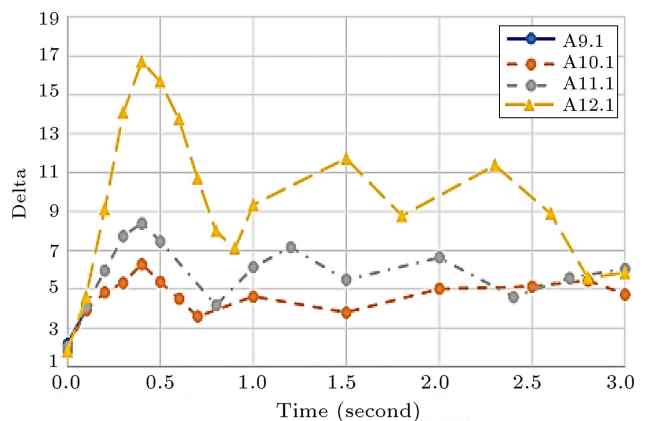
**Figure 10.** The graphs for water drop deformation in two-phase flow in the absence of gravity with the voltage of 3000 V.



**Figure 13.** Water drop deformation graph for two-phase flow in the absence of gravity for a drop radius of 7.5 mm and variable applied voltage.



**Figure 11.** The graphs for water drop deformation in two-phase flow in the absence of gravity with the voltage of 2000 V.



**Figure 14.** Water drop deformation graph for two-phase flow in the absence of gravity for a drop radius of 10 mm and variable applied voltage.

10, and 11 for constant voltage and Figures 12, 13, and 14 for constant radiuses and changing voltages. These results will be explained in the following section.

According to Figure 9, it can be seen that water droplet deformation increases with the increase in

droplet radius at a constant voltage of 5000 V which is evident from the starting section of the graphs.

The deformation of the water drop at the voltage of 2000 V (Figure 11) shows that the change in the applied voltage intensifies the deformation of the

droplet. Based on the data presented in the A2.1 graph, a drop with a radius of 5 mm shows the least amount of deformation at the applied voltage of 2000 V while graph A10.1 for a droplet radius of 10 mm shows that these deformations are at their maximum during the first second of the analysis, resulting to up to 6 mm of change in droplet diameter.

Based on the graphs presented in Figures 9 to 11 in this study, the increase in deformation is seen with an increase in drop diameter. As can be seen in these graphs, with an increase in the water drop's diameter, its deformation to an oval shape increases. In the next step, analysis graphs are compared for constant drop radius and changing the electrical voltage to determine the effect of the electrical field in two-phase water-oil flow in the absence of the earth's gravity.

Figures 12 to 14 show the deformation of various droplet radiuses at different applied voltages. As can be seen, for constant droplet radius, increasing the voltage results in increased deformation for 1 second but afterward, the changes don't show a specific trend. This can be due to changes in the electrical field.

Figures 13 and 14 show that an increase in the current results in increased deformation in the analysis graphs. This is most clear in the graphs for analyses A12.1 and A8.1, where changes in the voltage at constant drop radius have increased deformation by several times.

These results also indicate that the voltage with the highest deformation at a constant drop radius and in the absence of gravity is 5000 V.

As can be seen in the software analysis graphs of the water drop in the presence of an electrical field and the absence of gravity, an increase in the electrical field, and changes in the applied voltage can significantly affect the shape of the droplet. This confirms the first research hypothesis.

Furthermore, observations show a logical correlation between drop radius and the electrical field's voltage and this correlation is larger for larger drops at a constant voltage.

Another observation is that in all analyses, the simulation in the absence of gravity must continue for 3 seconds to reach the maximum deformation except for analysis A8.1 which requires 2.6 seconds to reach maximum deformation.

The second hypothesis states that the deformation speed decreases with an increase in the drop diameter. This change is relatively seen in the analysis results. However, the graph showing the absolute deformation of water drops is not able to identify these changes due to the heterogeneous conditions of the water droplets.

The changes in water drop deformation in software simulation in the presence of an electrical field and the earth's gravity are presented in the next section

which shows a significant difference compared to the case with the absence of gravity.

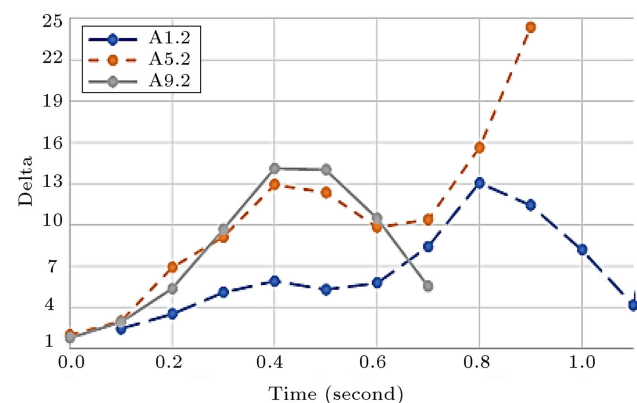
## 5.2. Water drop deformation in the presence of earth's gravity

The results of the analysis of water drop deformation in the presence of the earth's gravity are presented in Table 5.

Based on the table of the results for software analysis of two-phase water-oil flow under current conditions, it can be seen that the deformation shows an increasing trend at constant voltage and different droplet diameters from 5 mm to 10 mm. One important point of note for graphs obtained in the presence of gravity is that the presence of gravity not only results in the movement of the droplet but also leads to its unsymmetrical deformation. This results in a non-prismatic deformation of the droplet and some cases has disintegrated the droplet, creating several smaller droplets.

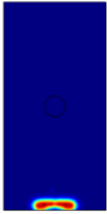
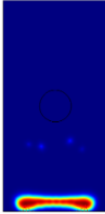
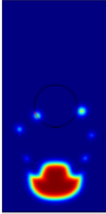
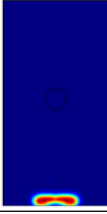
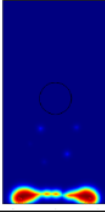
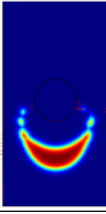
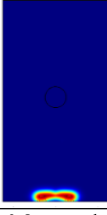
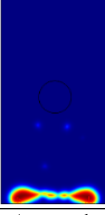
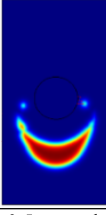

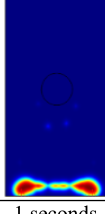
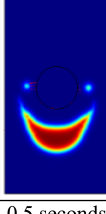
Another important fact observable in these figures is that, unlike analyses carried out in the absence of earth's gravity, the water droplet does not require a long time to disintegrate, leading to disintegration or satisfaction of one of the stop conditions within 1 second from the start of the analyses.

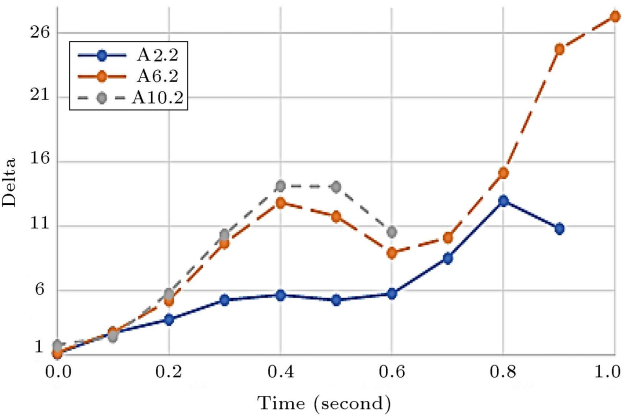
It is also important to note that an increase in the voltage of the electrical field has not resulted in changes in the disintegration time of the water droplet and has only resulted in an increase in water drop deformation during this time. This means that at the voltage of 1000 V, the analysis is stopped due to impact condition but this has changed to disintegration condition with an increase in the voltage. The graphs obtained from the analysis of the water drop in the presence of gravity are presented in the following section. Figures 15–18 show the deformation of a water drop in the presence of the earth's gravity at constant voltage. These results shall be discussed in the



**Figure 15.** Deformation graph for water drop in two-phase flow in the presence of gravity and voltage of 1000 V.

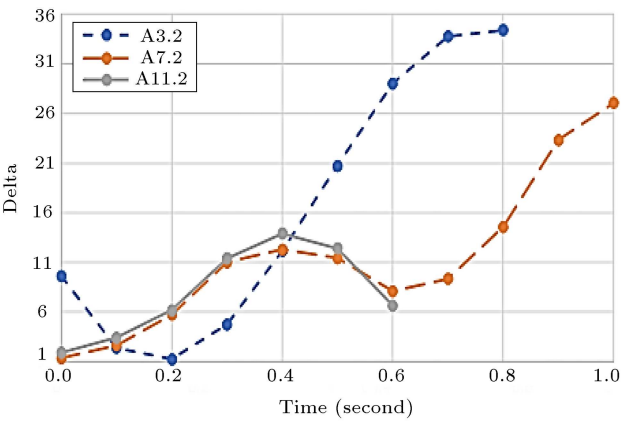
**Table 5.** Stopped-time water drop deformations in the presence of gravity.

| Voltage | Remarks | Drop radius   |  |   |
|---------|---------|---|--|---|
|         |         | 5 mm  | 7.5 mm   | 10 mm   |
| 1000    | Shape   |    |    |    |
|         | Time    | 0.8 seconds   | 0.9 seconds  | 0.7 seconds   |
| 2000    | Shape   |    |    |    |
|         | Time    | 0.8 seconds   | 1 seconds  | 0.5 seconds   |
| 3000    | Shape   |   |   |   |
|         | Time    | 0.8 seconds   | 1 seconds  | 0.5 seconds   |
| 5000    | Shape   |  |  |  |
|         | Time    | 0.9 seconds   | 1 seconds  | 0.5 seconds   |



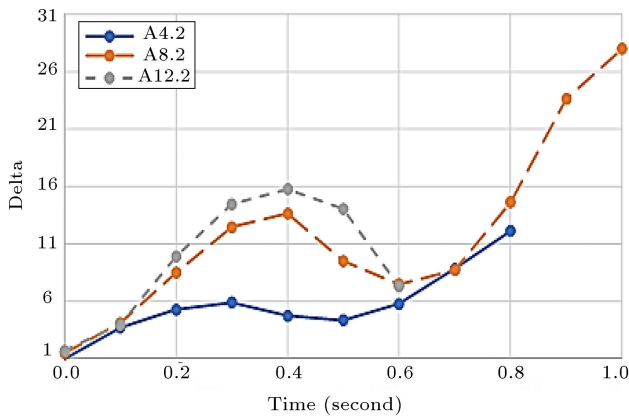
**Figure 16.** Deformation graph for water drop in two-phase flow in the presence of gravity and voltage of 2000 V.

following sections. Figure 15 shows that an increase in the water drop’s radius has resulted in an initial increase in deformation. However, the deformation then shows an inverse trend due to the effects of the



**Figure 17.** Deformation graph for water drop in two-phase flow in the presence of gravity and voltage of 3000 V.

electrical field on some water drop diameters. As can be seen, the deformation graphs for water drop radiuses of 5 mm and 10 mm decrease after some time while this decrease is not observed in the water

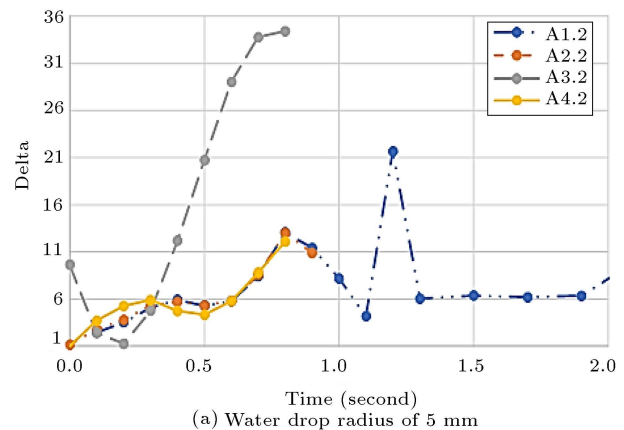


**Figure 18.** Deformation graph for water drop in two-phase flow in the presence of gravity and voltage of 5000 V.

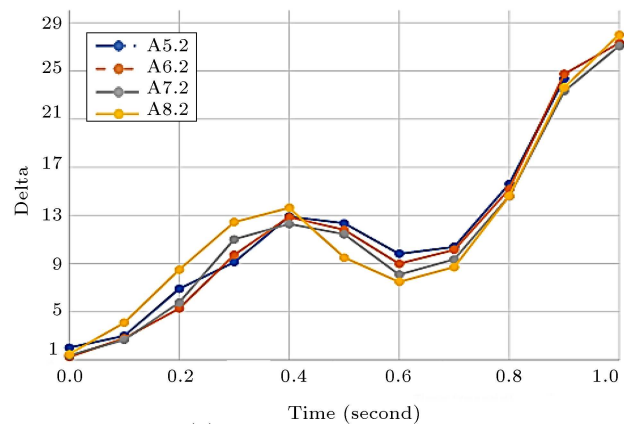
drop radius of 7.5 mm and the initial increasing trend has continued.

It is also worth noting that in Figure 15, the data are gathered in the presence of the earth's gravity for up to 1 second after which the water drop has satisfied the impact or disintegration conditions. Therefore, it can be said that the addition of gravity's effects results in more realistic problem conditions, distancing the results from the ideal initial experiment conditions. According to Figure 16, it can be seen that the general trend observed previously had been maintained for the water drop deformation in the presence of the earth's gravity and voltage of 2000 V. However, based on the slope of the graphs, it can be seen that the deformation trends for the water drop are more uniform in this case. Furthermore, in regards to analysis times, it can be observed that the total analysis time shows a significant decrease, reaching maximum deformation and stop conditions within at most 1 second from the start of the analysis.

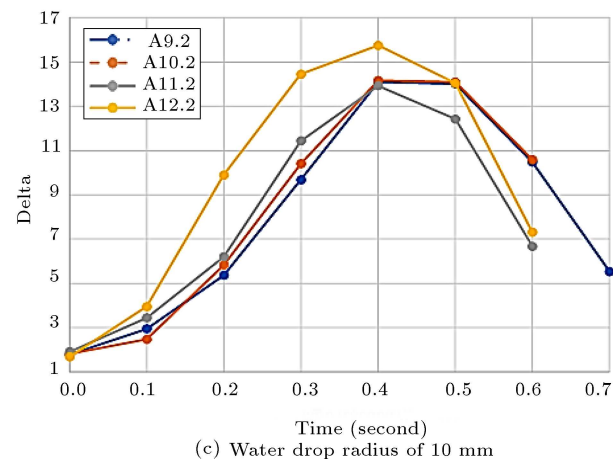
Figure 17 also shows that at the constant voltage, an increase in the water drop radius has resulted in greater deformation. Furthermore, the inversion of changes in deformation at certain times is also observed in the presence of gravity and a constant electrical field. Evaluation of these results indicates that this inversion in the water drop deformation is due to a similar alignment between electrical field conditions and water drop in the two-phase flow. Furthermore, the total analysis times observed in Figures 15 and 16 are maintained in this case as well, resulting in disintegration or impact of the water drop and satisfaction of stop conditions within 1 second. Based on the changes observed in the above graphs, it can be seen that at the radius of 7.5 mm, the water drop has shown maximum deformation which is more than twice the other cases for both A8.2 and A7.2 graphs. This shows a similar response to the electrical field with voltages of 3000 V and 5000 V for these two



(a) Water drop radius of 5 mm



(b) Water drop radius of 7.5 mm



(c) Water drop radius of 10 mm

**Figure 19.** Water drop deformation graph in the two-phase flow in the presence of gravity at different voltages.

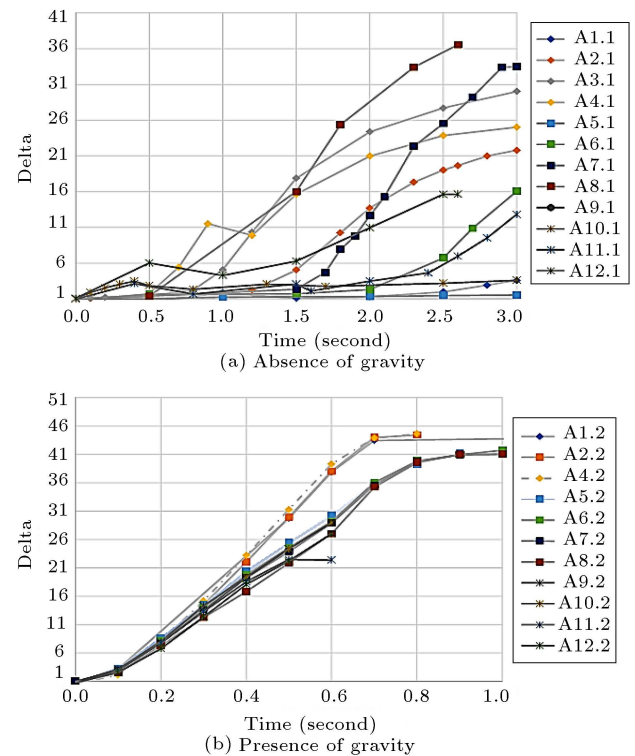
samples. However, the maximum deformation of the water drop in the A7.2 graph is 26 mm while the A8.2 graph shows a slight increase in total deformation, which can be due to the increase in the electrical field voltage. Figure 19, presented below, uses similar water drop radii and investigates the effects of changes in the electrical field under constant geometrical conditions.

Figure 19(a) shows the deformation of a water drop with a radius of 5 mm at different applied voltages. It can be seen that until close to 1 second, the analysis results at 3 different voltages show similar results while the analysis results for A3.2 are significantly higher, almost 1.5 times higher than other results. Another important fact is that the A1.2 analysis for an applied voltage of 1000 V shows deformation after 1 second but these deformations are not investigated due to the stop point at 1.2 seconds. Future studies can investigate this phenomenon and deformations after water drop disintegration which might result in the reformation of the water drop and return to the initial conditions. However, this part of the deformation has not been investigated in the current study. The following two figures show the deformation at different voltages for water drop radiuses of 7.5 mm and 10 mm.

Figures 19(b) and (c) show that, unlike what was observed in Figure 17, the response in different voltages has been almost identical for similar water drop radiuses and the deformation has followed a similar and logical path. However, Figure 19(b) for a water drop radius of 7.5 mm shows that the water drop has an almost entirely increasing deformation which is not present in Figure 19(c), in which, the drop with a radius of 10 mm has shown increasing deformation until 0.4 seconds after the start of the analysis without satisfying the spot conditions, after which the response under different applied voltages has been reversed, resulting in decreasing deformation of the water drop.

### 5.3. Investigating the water drop movement in the presence and absence of earth's gravity

Based on the results presented in the previous sections, it was observed that changes in the applied voltage and the water drop radius result in changes in the deformation in most cases and this deformation is significantly different in the presence and absence of the earth's gravity. Now, to compare these results, we can investigate the movement of a water drop, or in other words, its decentralization from its initial modeling position, under different problem conditions. To this end, in the current study, the decentralization of the water drop in the presence and absence of the earth's gravity was investigated. The results indicated that for graphs under the effect of gravity, the velocity of water drop movement is significantly higher while other problem conditions including changes in the voltage of the electrical field applied to the two-phase low as well as changes in the water drop radius also play important roles. In regards to satisfying the stop conditions, the results indicated that the stop times decrease to approximately 30% of their initial value in the presence of the earth's gravity. This indicates that



**Figure 20.** Movement of water drop in the two-phase flow at various radiuses and voltages.

phenomena occurring under real conditions either don't occur during ideal numerical simulation conditions or are slow to manifest. Figure 20 shows the changes in the position of the water drop relative to the center in the presence and absence of gravity.

According to Figure 20 and analysis of the data obtained in the presence and absence of the earth's gravity, it can be seen that the movement velocity of the water drop shows a significant increase when gravity is present in the problem. As a result, in the absence of gravity, the water drop needs approximately 3 seconds to satisfy stop conditions and these conditions have not even been met in some cases. However, as can be seen in Figure 20(b), the movement is significantly faster in the presence of gravity and the stop conditions have been satisfied 30% of the time required in the absence of gravity. Another change relates to the movement of water drop in two-phase flow due to the changes in the electrical field. In the case without gravity, the changes are random and do not follow a logical trend. However, Figure 20(b), showing graphs in the presence of the earth's gravity, shows a logical and almost constant trend of changes with changes in the water drop radius, and the water drop's movements are almost equal for equal radiuses.

## 6. Conclusion

After evaluating the graphs extracted from the results

of software analyses and linear regression results, several conclusions can be reached which are presented as follows.

The time of analysis was equal in all simulations with and without the presence of gravity. In the cases with the gravity applied to the numerical model, the analysis time continued until stop conditions were satisfied. In some of the analyses, stop conditions were not satisfied at the end of modeling time but in cases where earth's gravity was applied to the modeling, maximum analysis time was limited to 1 second. This however was not universally true for all cases and, even in the absence of gravity, some analyses showed a reduction in analysis time and reached stop conditions. It can be theorized that in these cases, the two-phase flow is aligned with the electrical field, resulting in a shortening of analysis time and quickly satisfying stop conditions.

1. In regards to the effect of changes in water drop radius at constant voltage, the results indicate that in general, an increase in initial radius results in an increase in deformation of the water drop except in cases where the electrical field is insufficient for deformation such as analysis A9.1 which showed no significant deformation of the water drop in the electrical field after 3 seconds;
2. Changes in the voltage at a constant initial water drop radius indicate that changes in voltage have significant effects on the deformation of the water drops. According to these results, while total analysis and stop times show no significant changes, the main effect of voltage had been on the water drop deformation. Some analyses even show water drops deforming to the shape of an elongated rod covering the entire width of the oil medium;
3. The effects of the presence or absence of the earth's gravity were also among the significant results of these analyses. According to the results, in the presence of gravity, analysis time has decreased to approximately 30% of the initial 3-second analysis time. Normally, in the absence of the earth's gravity, deformations are limited, and visible changes in the two-phase flow are limited to the movement of the water droplets inside the oil medium. However, in the presence of the earth's gravity, the water drop quickly deforms in less than 1 second, experiencing both deformation and movements in the two-phase environment;
4. Finally, the results of the current study indicate that changes in the geometrical radius, as well as voltage, have affected the movement of water drops in both cases with or without the presence of the earth's gravity. However, water drop deformation in the presence of gravity had been significantly higher

compared to the case with the absence of gravity and this deformation has increased with an increase in the electrical field's voltage. In other words, it can be said that including the earth's gravity in calculations brings the results closer to real results compared to the cases without the presence of gravity.

### Data available

The data that support the findings of this study are available from the corresponding author upon reasonable request.

### References

1. Hosseini, E., Aghadavoodi, E., Shahgholian, Gh., et al. "Intelligent pitch angle control based on gain-scheduled recurrent ANFIS", *Journal of Renewable Energy and Environment*, **6**(1), pp. 36–45 (2019).
2. Emamdad, M., Akbari, E., Karbasi, S., et al. "Design and analysis of a new structure for non-isolated dc-dc boost converters", *Journal of Intelligent Procedures in Electrical Technology*, **15**(58), pp. 109–120 (2024).
3. Sattar, M., Samiei-Moghaddam, M., Azarfar, A., et al. "Joint optimization of integrated energy systems in the presence of renewable energy sources, power-to-gas systems and energy storage", *Journal of Intelligent Procedures in Electrical Technology*, **15**(57), pp. 15–30 (2024).
4. Sadeqi, S., Xiros, N., Aktosun, E., et al. "Power estimation of an experimental ocean current turbine based on the conformal mapping and blade element momentum theory", ASME International Mechanical Engineering Congress and Exposition, Paper no: IMECE2021-71751, V07BT07A004; 9 pages (2022).
5. Samadi-Darafshani, M., Safavi, H.R., Golmohammadi, M.H., et al. "Assessment of the management scenarios for groundwater quality remediation of a nitrate-contaminated aquifer", *Environmental Monitoring and Assessment*, **193**(4), pp. 1–16 (2021).
6. Mortazavi, M., Yaghoubi, S., and Jahangiri, M. "Investigating the effect of buffer tank type on technical and environmental performance of solar heating systems in Iran", *International Journal of Smart Electrical Engineering*, **11**(02), pp. 55–61 (2022).
7. Yaghoubi, S., Shirani, E., and Pischevar, A. "Improvement of dissipative particle dynamics method by taking into account the particle size", *Scientia Iranica*, **26**(3), pp. 1438–1445 (2019).
8. Borhani, M. and Yaghoubi, S. "Improvement of energy dissipative particle dynamics method to increase accuracy", *Journal of Thermal Analysis and Calorimetry*, **44**, pp. 2543–2555 (2021).
9. Borhani, M. and Yaghoubi, S. "Numerical simulation of heat transfer in a parallel plate channel and promote dissipative particle dynamics method using different

- weight functions”, *International Communications in Heat and Mass Transfer*, **115**, 104606 (2020).
10. Hedarpour, F. and Shahgholian, G. “Stability improvement of hydraulic turbine regulating system using round-robin scheduling algorithm”, *Journal of Renewable Energy and Environment*, **5**(1), pp. 1–7 (2018).
  11. Atten, P. “Electrohydrodynamics of dispersed drops of conducting liquid: From drops deformation and interaction to emulsion evolution”, *Int. J. Plasma Environ. Sci. Technol.*, **7**(1), pp. 2–12 (2013).
  12. Abbasi, M.S., Song, R., Cho, S., et al. “Electrohydrodynamics of emulsion droplets: Physical insights to applications”, *Micromachines*, **11**(10), p. 942 (2020).
  13. Vlahovska, P.M. “Electrohydrodynamics of drops and vesicles”, *Annual Review of Fluid Mechanics*, **51**(1), pp. 305–330 (2019).
  14. Sjöblom, J., Mhatre, S., Simon, S., et al. “Emulsions in external electric fields”, *Advances in Colloid and Interface Science*, **294**, 102455 (2021).
  15. Mandal, S., Bandopadhyay, A., and Chakraborty, S. “The effect of uniform electric field on the cross-stream migration of a drop in plane Poiseuille flow”, *Journal of Fluid Mechanics*, **809**, pp. 726–774 (2016).
  16. Mandal, S., Sinha, S., Bandopadhyay, A., et al. “Drop deformation and emulsion rheology under the combined influence of uniform electric field and linear flow”, *Journal of Fluid Mechanics*, **841**, pp. 408–433 (2018).
  17. Yoshimoto, H., Shin, Y.M., Terai, H., et al. “A biodegradable nanofiber scaffold by electrospinning and its potential for bone tissue engineering”, *Biomaterials*, **24**(12), pp. 2077–2082 (2003).
  18. Gañán-Calvo, A. “Erratum: cone-jet analytical extension of Taylor’s electrostatic solution and the asymptotic universal scaling laws in electrospraying”, *Phys. Rev. Lett.*, **85**, p. 4193 (2000).
  19. Eow, J.S., Ghadiri, M., Sharif, A.O., et al. “Electrostatic enhancement of coalescence of water droplets in oil: a review of the current understanding”, *Chemical Engineering Journal*, **84**(3), pp. 173–192 (2001).
  20. Guo, C. and He, L. “Coalescence behavior of two large water-drops in viscous oil under a DC electric field”, *J. Electrostat.*, **72**, pp. 470–476 (2014).
  21. Cho, S.K., Moon, H., and Kim, C.J. “Creating, transporting, cutting, and merging liquid droplets by electrowetting-based actuation for digital microfluidic circuits”, *Journal of Microelectromechanical systems*, **12**(1), pp. 70–80 (2003).
  22. Vizika, O. and Saville D.A. “The electrohydrodynamic deformation of drops suspended in liquids in steady and oscillatory electric fields”, *Journal of Fluid Mechanics*, **239**, pp. 1–21 (1992).
  23. Saville, D. “Electrohydrodynamics: the Taylor-Melcher leaky dielectric model”, *Annual Review of Fluid Mechanics*, **29**(1), pp. 27–64 (1997).
  24. Eow, J.S. and Ghadiri, M. “Motion, deformation and break-up of aqueous drops in oils under high electric field strengths”, *Chemical Engineering and Processing: Process Intensification*, **42**(4), pp. 259–272 (2003).
  25. Yan, H., He, L., Luo, X., et al. “Investigation on transient oscillation of droplet deformation before conical breakup under alternating current electric field”, *Langmuir*, **31**(30), pp. 8275–8283 (2015).
  26. Huang, X., He, L., Luo, X., et al. “Deformation and coalescence of water droplets in viscous fluid under a direct current electric field”, *International Journal of Multiphase Flow*, **118**, pp. 1–9 (2019).
  27. Li, B., Dou, X., Yu, K., et al. “Electrocoalescence of water droplet trains in sunflower oil under the coupling of non-uniform electric and Laminar flow fields”, *Chemical Engineering Science*, **248**, 117158 (2022).
  28. Li, B., Dou, X., Yu, K., et al. “Coalescence dynamic response of an aqueous droplet at an oil-water interface under a steady electric field”, *International Journal of Multiphase Flow*, **139**, 103628 (2021).
  29. Gong, H., Liao, Z., Peng, Y., et al. “Numerical simulation of dynamic characteristics of droplet in oil under a CPPM electric field”, *Chemical Engineering Science*, **248**, 117248 (2022).
  30. Li, N., Sun, Z., Sun, J., et al. “Deformation and breakup mechanism of water droplet in acidic crude oil emulsion under uniform electric field: A molecular dynamics study”, *Colloids and Surfaces A: Physicochemical and Engineering Aspects*, **6**(2), 127746 (2022).
  31. Li, N., Sun, Z., Liu, W., et al. “Effect of electric field strength on deformation and breakup behaviors of droplet in oil phase: A molecular dynamics study”, *Journal of Molecular Liquids*, **333**, 11599 (2021).
  32. Mittal, H.V.R., Ray, R.K., Gadêlha, H., et al. “A coupled immersed interface and level set method for simulation of interfacial flows steered by surface tension”, *Experimental and Computational Multiphase Flow*, **3**(1), pp. 21–37 (2021).
  33. Ostahie, C.N. and Sajin, T. “Kinetics of mechanical impurities electroseparation from dielectric liquids”, *Journal of Electrostatics*, **71**(4), pp. 695–702 (2013).
  34. Eow, J.S., Ghadiri, M., and Sharif, A.O. “Electrostatic and hydrodynamic separation of aqueous drops in a flowing viscous oil”, *Chemical Engineering and Processing: Process Intensification*, **41**(8), pp. 649–657 (2002).
  35. Mhatre, S., Vivacqua, V., Ghadiri, M., et al. “Electrostatic phase separation: A review”, *Chemical Engineering Research and Design*, **96**, pp. 177–195 (2015).
  36. O’Konski, C.T. and Thacher Jr, H.C. “The distortion of aerosol droplets by an electric field”, *The Journal of Physical Chemistry*, **57**, pp. 955–958 (1953).
  37. Taylor, G. “Disintegration of water drops in an electric field”, *Proceedings of the Royal Society of London, Series A. Mathematical and Physical Sciences*, **280**, pp. 383–397 (1964).

38. Basaran, O.A. and Scriven, L. "Axisymmetric shapes and stability of pendant and sessile drops in an electric field", *Journal of Colloid and Interface Science*, **140**, pp. 10–30 (1990).
39. Allan, R. and Mason, S. "Particle behaviour in shear and electric fields I. Deformation and burst of fluid drops", *Proceedings of the Royal Society of London, Series A. Mathematical and Physical Sciences*, **267**, pp. 45–61 (1962).
40. Baygents, J.C., Rivette, N.J., and Stone, H.A. "Electrohydrodynamic deformation and interaction of drop pairs", *Journal of Fluid Mechanics*, **368**, pp. 359–375 (1998).
41. Tadros, T., Izquierdo, P., Esquena, J., et al. "Formation and stability of nano-emulsions", *Advances in Colloid and Interface Science*, **108**, pp. 303–318 (2004).
42. Masmoudi, H., Piccerelle, P., Le Dréau, Y., et al. "A rheological method to evaluate the physical stability of highly viscous pharmaceutical oil-in-water emulsions", *Pharmaceutical Research*, **23**(8), pp. 1937–1947 (2006).
43. Martínez-Palou, R., de Lourdes Mosqueira, M., Zapata-Rendón, B., et al. "Transportation of heavy and extra-heavy crude oil by pipeline: A review", *Journal of Petroleum Science and Engineering*, **75**(3–4), pp. 274–282 (2011).
44. Osher, S. and Sethian, J.A. "Fronts propagating with curvature-dependent speed: Algorithms based on Hamilton-Jacobi formulations", *Journal of Computational Physics*, **79**(1), pp. 12–49 (1988).
45. Torza, S., Cox, R.G., and Mason, S.G. "Electrohydrodynamic deformation and bursts of liquid drops", *Philosophical Transactions of the Royal Society of London, Series A, Mathematical and Physical Sciences*, **269**(1198), pp. 295–319 (1971).

## Biographies

**Mehdi Taghian** obtained his BS and MS degrees at Najafabad Branch, Islamic Azad University, Najafabad, Iran. His research interest is modeling and numerical simulation. He is currently trying to become a doctoral student. His research interests are renewable energies, biofluid simulation, modeling of particle transport, and CFD simulations.

**Somaye Yaghoubi** obtained her BS, MS, and PhD degrees at Isfahan University of Technology, Iran, and is currently an Associate Professor of Mechanical Engineering at Najafabad Branch, Islamic Azad University, Najafabad, Iran. Her research interests are renewable energies, biofluid simulation, modeling of particle transport, and CFD simulations.